On Wafer Thin Micro Batteries: Micro-fabrication, Towards the Development of Aluminum-anode High Performance Cells

J. Dlutowski, W. Moreno & M. Calves
University of South Florida
Department of Electrical Engineering
4202 E. Fowler Avenue; ENB 118
Tampa, FL 33620

A. M. Cardenas-Valencia
SRI International
Engineering Systems Division
450 8th Avenue SE
St. Petersburg, FL 33701

Abstract *— Reduction in size and weight of micro-electronic devices becomes limited by the availability of suitable power sources. This paper presents micro-fabrication routes of an aluminum anode/oxygenated alkaline electrolyte/platinum cathode micro cell as a first step towards the development of highly efficient thin form factor aluminum anode cells. On-demand microfluidic addition of electrolyte can offer long shelf life. Several cell designs are made on a single wafer allowing for variation of the electrode area ratio; this ratio affects the aluminum anode utilization efficiency. Cell's open circuit voltages are in the 1.2-1.4 Volt range. Several geometries provide high current densities relative to the cell's overall size when subject~~ed~~ to small load resistances (up to 2 milliamps per cm^2). A preliminary comparison of anode utilization efficiencies (energy per unit gram of deposited aluminum) among fabricated cells with various platinum aluminum area ratios is presented.*

I. INTRODUCTION

The development of Micro-electromechanical Systems (MEMS) has enabled the design of portable sensor systems that require reliable powering systems of comparable sizes. Parallel development of small but highly efficient powering devices is required. Power-MEMS is still an area of active research and development [1-2]. Reports on micro and miniature energy environmental harvesting systems and thermal and combustion devices are common in literature [1-6]. A variety of electronic devices, from cell phones and lap top computers to medical devices rely on the use of batteries. A logical approach is the miniaturization of electrochemical cells [7-16] as a Power-MEMS option. Lithium-ion thin film batteries were one of the first systems to be investigated for the development of micro batteries [8-11]. Fuel and semi-fuel cells are also subjects of miniaturization [12-14].

Microfabricated galvanic cells in which "activation on demand" via micro fluidic actuation of electrolytes has also been investigated [12-18]. While the proposed cells are not rechargeable, the on-demand concept is attractive, as it overcomes the known degradation over time that most available commercial batteries experience, and provides a disposable device alternative for Power-MEMS.

Results for an aluminum/air semi-fuel cell, formed by layering polymeric and metallic materials, were also previously published by our research group [13]. A thermo-pneumatic actuation mechanism –where, upon heating, a working fluid expands pushing the electrolyte solution– constituting the micro-fluidic actuation, was reported. A second report [14] included a Daniell (Copper-Zinc) electrochemical battery, where each metal electrode compartment contained solutions of its ion salts. The cell activation was proposed via a polyacrylamide swellable polymer that, upon the release of a saline solution, will expand and close the cell circuit. More recently, an electrolytic bubbler was explored to induce the fluidic actuation, to further reduce the activation energy [15]. The addition of hydrogen peroxide to an alkaline electrolyte and other aluminum anode chemistries, coupled either with air or alkali peroxide, conferred higher energetic densities, and were also presented.

Other groups have also reported on fabricating cells whose activation can potentially be achieved by the dispensing of electrolytes. Lee and Lin [16] reported on micro

batteries on a silicon substrate. On top of a nitride passivation layer, alternating PSG (phosphosilicate glass) sacrificial layers and polysilicon layers were patterned in order to form a cavity. A 600x850 um gold electrode was deposited using a lift-off technique. Sulfuric acid and hydrogen peroxide constitute the electrolyte. Sammoura et al [17] developed microbatteries via a two-wafer design. AgCl or CuCl was sputtered to form the cathode. The top wafer is etched using Deep Reactive Ion Etching (DRIE) to provide openings for electrolytes to enter the cell. Magnesium was sputtered onto the bottom side of the wafer to form the anode.

Herein, the fabrication using standard MEMS processes of on-wafer, aluminum anode, galvanic cells is presented. Challenges (adhesion) and resulting process modifications, as well as details about the process conditions and final dimensions of each layer are reported in this paper. Additionally, a preliminary set of performance results that include calculations of energetic content in the cells is presented.

II. OPTIMIZATION OF ALUMINUM UTILIZATION VIA ELECTRODE AREA RATIO

A. *Chemistry*

The oxidation potential of aluminum in alkaline solutions is +2.3 Volts when aluminum changes its oxidation state by three electrons. When these aluminum electrochemical properties are considered along with the low density and atomic weight, theoretical energy densities of aluminum anodes make the use of its chemistries very desirable as an alternative power source (17-24 kJ/gram of aluminum). This fact justifies the intense research activity that has taken place on coupling aluminum with various electrolytes [18-22]. The preferred electrochemical reaction in aluminum anode alkaline cells, in the presence of hydrogen peroxide, $H_2O_{2\,(l)}$ is

$$2Al_{(s)} + 3H_2O_{2(aq)} + 2OH^{-1}{}_{(aq)} \rightarrow 2Al(OH)_4{}^{-1}{}_{(aq)}. \quad (1)$$

In alkaline solutions, in the presence of hydrogen peroxide, competing reactions reduce aluminum anode performance. These reactions, together with over-potential effects (the required voltage to overcome cell internal processes for the charge transfer to occur), reduce the cell energy output well below the theoretical value. One of these competing reactions is known as direct reaction, and takes place when aluminum reacts with hydrogen peroxide to produce aluminum hydroxide. A competing reaction that also produces aluminum hydroxide in addition to hydrogen gas is corrosion.

The desired cathode reaction, which must take place, for eq. 1 to occur is

$$H_2O_{2(aq)} + OH^{-1}{}_{(aq)} + 2\varepsilon \rightarrow 3OH^{-1}{}_{(aq)}. \quad (2)$$

However, hydrogen peroxide decomposition may also occur, where oxygen and water are formed. The release of gases is an issue in these galvanic cells as bubbling interferes with the electrochemical reactions. Aluminum hydroxide scales form around the anode as the alkali hydroxide is depleted, causing interference with eq. 1.

Only in the presence of the hydroxide ion, is the hydrogen peroxide hydrolyzed. This is the initial step in a mechanism in which the overall reaction is eq. 2. Balance of the cathode reaction, as a way to control the hydroxide ions concentration, has been proposed as a viable way to potentially lead to optimum energy output from the galvanic cell. Furthermore, this balancing can be achieved by using a larger cathode area compared to that of the aluminum area [21]. In this paper, a micro fabrication process is proposed to produce cells with varying area ratios, without the need of forming cavities via wafer bonding. Furthermore the cell's testing constitutes a preliminary investigation of the effect of the electrode area ratio on the cells performance.

B. *Mask Design*

This design allows for easy variation of the electrode area ratios via photo-patterning. In this work, the line width, as well as the cell configuration to achieve various platinum-to-aluminum area ratios, have been varied. Testing will determine if the cathode surface with respect to that of the aluminum can potentially benefit the aluminum utilization. In addition, the effect of device geometry is observed. To that end, nine different cell designs were incorporated, consisting of various "mesh" and "ring" configurations. Fig. 1 shows the various designs used in this work. Table 1 provides the

geometric details of each cell. A cross sectional view is shown in section III.

Copies of each of these cell designs were placed at various locations across the wafer to minimize the effects that preferred deposition on certain areas of the wafer (were this to occur in any of the deposition steps) could potentially have on cell performance. The mask was designed in a manner that each 100 mm diameter wafer would host 26 cells.

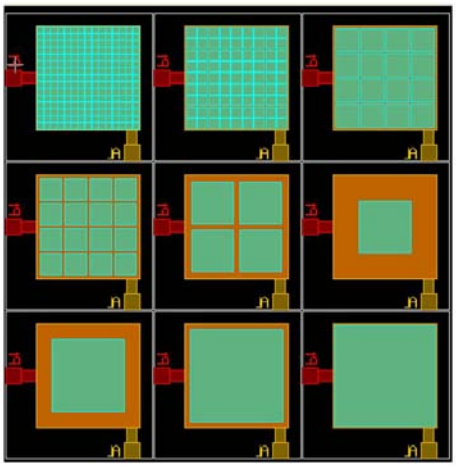

Figure 1. Various cell designs. Note cells 1-3 are on the top row, 4-6 on the middle and 7-9 on the bottom.

Cell ID	Ratio	Line Width (micrometers)
1	8.35	34.5
2	4.26	100
3	4.26	200
4	2.40	320
5	1.78	660
6	0.33	2500
7	0.96	1500
8	4.26	500
9	15.92	150

TABLE I. CELL GEOMETRY

III. MICRO FABRICATION PROCESS DEVELOPMENT

The process begins with <100>, 100mm diameter silicon wafers. The crystal orientation and doping concentration is inconsequential to device operation. The wafers were cleaned with acetone, followed by methanol and deionized water, and spun dry. A low stress, 300 nm thick silicon nitride layer was deposited in a Tystar LPCVD furnace at 835°C for 60 minutes with NH_3 flow rate of 20 scm. Negative photoresist (Futurex NR9-1000PY) was spun onto the wafer at 3000 RPM for 40 seconds, followed by a 150°C pre-exposure bake for 1 minute. Using a mask created to pattern the platinum electrodes and an EVG alignment system, the photoresist was exposed for 11 seconds, followed immediately by a post-exposure bake at 100°C for 1 minute. After allowing the wafer to cool down, the resist was developed in the Futurex RD-6 photoresist developer. After rinsing and spinning dry, the wafer was subjected to heat treatment for another minute at 100°C to drive out any moisture associated with the development process.

In initial attempts, platinum was deposited directly on the silicon nitride passivation layer. Delamination occurred either immediately during the lift-off step or after subsequent processing, regardless of the lift-off technique used (acetone or photoresist remover). Therefore an additional deposition of an adhesion layer was added. Using an AJA model ATA1800 sputtering system, a 10 nm titanium nitride layer was deposited. Deposition time was 3 minutes with RF power set at 360 W, argon flow rate at 29.4 scm, nitrogen flow at 2.6 scm and chamber pressure set at 2 mTorr. This part of the process was modified to test different adhesion layers. Aluminum nitride was deposited with the same power and pressure settings in the AJA sputtering system. Gas flow rates were also 29.4 scm for argon and 2.6 scm for nitrogen. Deposition time was 2 minutes.

In another variation, a 10 nm adhesion layer of silicon was deposited for 2 minutes in an argon plasma using a sputtering system built in-house. The Argon flow rate was 30 scm, RF power was 160W, and chamber pressure was 2 mTorr. Using this same sputtering system, silicon dioxide was deposited. Power and pressure settings were the same as silicon, flow rates were 26 scm for argon and 6 scm for oxygen. Deposition time was 6 minutes. All sputtered depositions were performed at room temperature.

Following the deposition of the adhesion layer, 100 nm of platinum were deposited using the in-house sputtering system for 4 minutes. Flow rate was 30 scm for argon at a pressure of 2mTorr. Lift-off of the platinum was performed using **a** type 1165 photoresist stripper at 80°C. Lift-off times were 15 minutes for the wafers with the silicon and silicon dioxide adhesion layers, 20 minutes for the wafer with the titanium nitride adhesion layer and over 90 minutes for the wafer with aluminum nitride. (Acetone was eventually used in the process after it was ruled out as the cause of delamination.) Upon completion of the lift-off process, the wafer was cleaned with isopropanol and deionized water and spun dry. The wafer with the silicon dioxide adhesion layer was delaminated and did not get processed further.

Next, a 500nm silicon dioxide layer was deposited in a Unaxis 790 PECVD (plasma enhanced chemical vapor deposition).

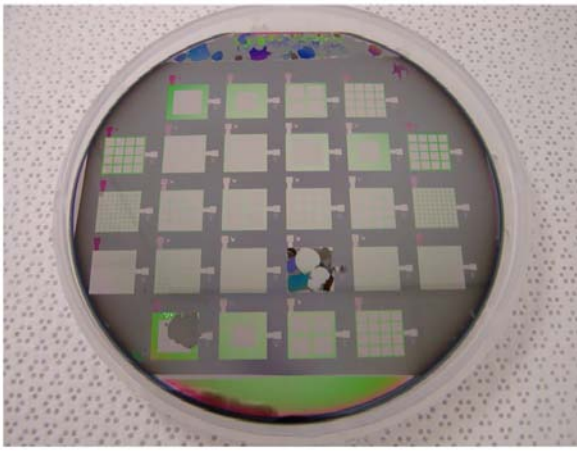

Figure 2. Original process showing patterned oxide where aluminum was expected as well as delaminated platinum

Substrate temperature was 250°C and deposition occurred for 10.5 minutes. The substrate was cooled to 150°C prior to its removal from the chamber.

In the initial attempts, a lift-off process similar to that used for platinum patterning was used for the aluminum deposition. This also resulted in delamination of the aluminum, leaving only the patterned silicon dioxide layer behind (see Fig. 2). An adhesion layer here could potentially affect the operation of the batteries, so the process was updated to etch the aluminum instead.

Using the in-house sputtering system, aluminum was deposited. Again, the argon flow rate was 30 scm. Deposition time was 30 minutes. Aluminum thickness was measured to be 30 nm ± 10% after the etch step using a Tencor profilimeter. Following aluminum deposition, positive photoresist (Shipley 1813) was spun onto the wafer at 3000 RPM for 40 seconds, followed by a 1 minute bake at 90°C. The pattern was aligned and exposed for 1.8 seconds, then developed for 40 seconds in MF 319. The wafer was then rinsed in deionized water and spun dry. The aluminum was etched in aluminum etchant for 8 minutes, under continuous agitation. Upon etch completion, the wafer was rinsed with deionized water and spun dry. The photo resist was then removed using **a** Shipley 1165 photoresist stripper at 80°C for 8 minutes, followed by rinse with isopropanol and deionized water and spun dry. (Note: the process was updated. The photoresist can be removed by spinning at 3000 rpm for 40 seconds with acetone followed by methanol.)

The oxide was etched in a Unaxis 790 RIE system. Etch time was 13 minutes. The platinum electrode acted as an etch stop and the aluminum electrode acted as a mask, preserving the oxide directly under the aluminum electrode. The resulting devices had a total electrode area of 1 cm^2 each. Fig. 3 shows a schematic cross section, as well as a solid model of one of the cells of the device.

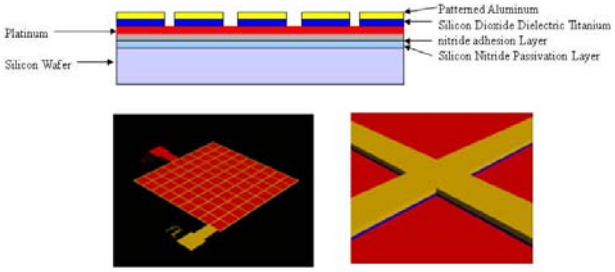

Figure 3. Cross section and solid model of typical cell. Close-up shows the silicon dioxide layer supporting the aluminum grid.

IV. Testing Protocol and Experimental Results

Contact was made to the aluminum and platinum electrodes using a probe station. The initial testing set consisted in subjecting 4.3-Pt:Al area-ratio cells with various ohm loads (no

load, 50 ohms, 100 ohms and 500 ohms). The very small amount of aluminum was expected to react quickly, limiting the life of the cells. The output voltage was monitored by taking data every second with a Fluke 180 logging multimeter. Cells were individually activated using 60 µl of a 1M NaOH solution to which 1 part hydrogen peroxide solution per 9 parts of solution was added.

Further testing was conducted in all of the fabricated cells, where a 100 ohm load was placed across the terminals. As described previously, voltage data as a function of time was recorded after the electrolyte was introduced onto each cell. Instantaneous current and power were calculated from the voltage data and then numerically integrated with respect to time to obtain the current and energy capacity of the cells. Power per gram of aluminum was determined using the area ratios of each cell and the average aluminum thickness of 300 nm.

Cell Performance

Fig. 4 shows the voltage output achieved for replicates of Cell ID #2 (4.3 area ratio) subjected to various loads. Note that as more current is drawn from the cell, the potential decreases, evidence of the existence of overpotentials. The potentials shown in the figure are easily measurable with the multimeter used and these results confirmed that testing can continue for all the cells exclusively with the 100 ohm-load. Fig. 4 also shows various replicates using a 100-ohm-nominal-load which shows the consistency in the obtained data for different cells.

Fig. 5 compares device efficiency for each cell ID with the various adhesion layers. Each set of data shows a trend with the device efficiency being low at low area ratios and becoming asymptotic as the ratio increases. It should be noted that cell ID 8 and 9 (with the ring configuration) did not survive any of the testing (ultra low output) and are not included in these results.

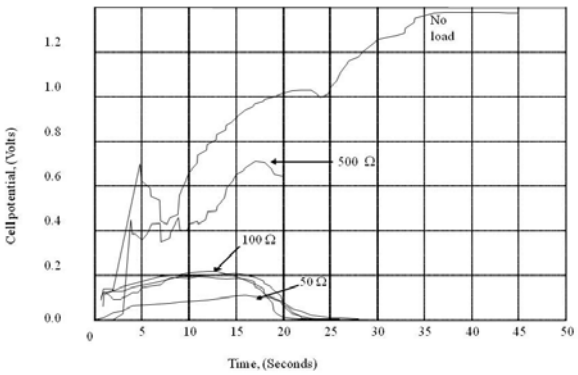

Figure 4. Output of 4.3 area ratio cells under various loads, including multiple replicates under 100 ohm load.

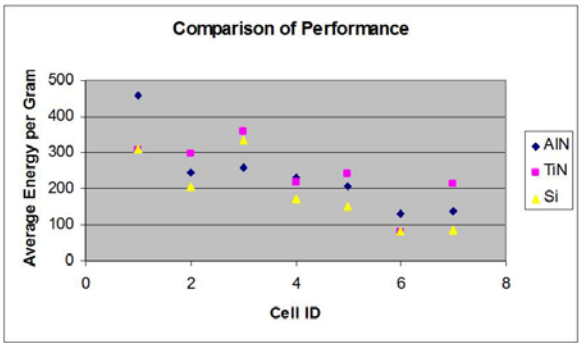

Figure 5. Performance Comparison – Note that cells with higher area ratios (cells ID 1 to 3) tend to have significantly higher energy per gram of Al, regardless of the adhesion material used. Cell geometry data is shown in Table 1. No replicates of cells 8 and 9 produced results.

Note that the various adhesion layers do not have an apparent relevant effect on device performance. This, together with the difficulty of performing lift-off on the wafers with the aluminum nitride adhesion layers led to the decision to proceed using titanium nitride. It is also evident that cells 1 through 3 exhibit significantly higher efficiencies than the other cells.

V. Conclusions and Ongoing Work

The process development for creating aluminum anode, platinum cathode microbatteries on a single passivated silicon wafer is described. The finalized process is

presented in detail, highlighting some difficulties encountered in early attempts. Due to the relative processing ease of titanium nitride, this is the most promising adhesion material. The adhesion material was not expected to have an effect on device performance, and results for all tested cells (for a given device ID) were all within the observed variability for the other cells. All tests indicate that high area ratios of platinum to aluminum produce better device efficiencies, but further experimentation is required to determine if the width of the grid lines affect device efficiency. However, it was shown that a grid-like anode geometry performed significantly better than ring-like geometries.

REFERENCES

[1] P. B. Koeneman, I. J. Busch-Vishniac and K. L. Wood, Feasibility of micro power supplies for MEMS, J. Microelectromech. Syst., Vol. 6 No. 4, (1997) 355-362.

[2] D. Pescovitz, The Power of Small Tech, Small times, Publisher Steve Crosby, Ann Arbor, MI, Jan/Feb, (2002) 21-31.

[3] Lee, J. B. Chen, Z., Allen M. G., Rohatgi, A. and Arya, R. A miniaturized High-voltage Solar Cell array as an electrostatic MEMS Power supply. J. microelectromech. Systems. 4 102-108, 1995.

[4] Roundy, S., Wright, P. K., and Pister, K. S. J., 2002, Micro-electrostatic Vibration-to-electricity Converters, *Proc. ASME International Mechanical Engineering Congress and Exposition, IMECE 2002*, New Orleans, LA, Vol. 2, IMECE2002-39309.

[5] Whalen, S. A., Thompson, M. R. Richards, C. D., Bahr, D. F. and Richards, R. F. Low Frequency operation of the P-3 micro heat engine. Proc. Of IMECE 2002. ASME International Mehcnaical Engineering Congress & Exposition. Nov. 17-22, New Orleans, Lousiana.

[6] W. Yang, S. K. Chou, C. Shu, H. Xue, and Z. Li, Design, Fabrication and Testing of a Prototype Microthermophotovoltaic System. J. of Microelectromech. Syst. 13(5) 2004

[7] Itoigawa, K. Ueno, H., Msayoshi, S., Toshiyuki, T., and Sugiyama, S. Fabrication of flexible thermopile generator. J. icromech. And Microeng. 15 (2005) S233-S238.

[8] Bates, J. B. , Gruzalski, G.R. and Luck,C. F. Rechargable Solid-State Lithium microbatteries. Procedina IEEE Micro Electromechanical Systems (MEMS '93), Fort Lauderdale FL. 1993, p82-86.

[9] H S Moon, W S Ji, T J Kim, W I Cho, Y S Yoon, S H Chung, and J W Park, "Electrochemical properties of diamond-like-carbon coated $LiMn_2O_4$ thin films for microbatteries" vol 2, pp. 165-169, 2001

[10] W C West, J. F. Whitacre, V. White and B. V. Ratnakumar, Fabrication and Testing of all solid-state microscal lithium batteries for microspacecraft applications. J. Micromech. Microeng. 12 (2002) 58-62

[11] R Wartena, A E Curtright, C B Arnold, A Pique, and K E Swider-Lyons, "Li-ion microbatteries generated by a laser direct write method," J Power Sources, Vol 126, pp. 193-202, 2004.

[12] T. Pichonat and B. Gautier-Manuel. Development of porous silicon based miniature fuel cells. J. Micromech. Microeng. 15 (2005) S179-S184

[13] A.M. Cardenas-Valencia, V. R Challa, D. Fries, L. Langebrake, R. F. Benson and S. Bhansali. " A Microfluidic Galvanic Cell as an on-chip power source". *Sens. and Act*. B Vol. 95, 2003, pp. 406-413.

[14] A. M. Cardenas-Valencia, D. Fries, H. Broadbent, L. Langebrake, and R. F. Benson "Micro-actuated Aluminum Galvanic and semi-fuel cells for Powering Remote Lab on a Chip Applications" Proc. Volume, μTAS 2003, The 7th International Conference on Miniaturized Chemical and BioChemical Analysis Systems, Vol. 1 pp. 311-314

[15] A. M. Cardenas-Valencia; D. P. Fries; G. Steimle; H. Broadbent, L. C. Langebrake and Benson R. F. "Fabrication of micro-actuated galvanic cells as power sources for Lab on chip applications by means of novel PCB/MEMS technology". Paper presented and published in Proc of the First International Conference Fuel Cells, NY, USA on April 24-25, 2003.

[16] K.B. Lee, and L. Lin, "Electrolyte-based on-demand and disposable microbattery," J Microelectromechanical systems, Vol 12, pp. 840-847, 2003

[17] F. Sammoura, K.B. Lee, and L. Lin, "Water activated disposable and long shelf life microbatteries," Sensors and Actuators A: Physical Vol. 111(1) pp. 79-86 2004

[18] S. Licht, Novel aluminum batteries",Col. Surf. A, Vol. 134 No 1, pp. 241-248(1998).

[19] Q. Li, N. Bjerrum,"Al as anode for energy storage"J. Pow. Sourc.,110,pp.1-10 (2002).

[20] Yang, Shaohua, Knickle, Harold. Design and analysis of aluminum/air battery system for electric vehicles . Journal of Power Sources v 112 n 1 Oct 24 2002 p 162-173

[21] Brodrecht, David J., Rusek, John J., Aluminum-hydrogen peroxide fuel-cell studies Applied Energy v 74 n 1-2 January/February 2003 p 113-124 (one O got yesterday)

[22] R. Benson, A. Cardenas and L. Langebrake. High energy Galvanic Cell from Aluminum and Alkali Metal peroxide. Provisional Patent granted USF. Currently non provisional Patent pending